JOURNAL OF MATERIALS SCIENCE **36** (2001) 4711–4717

Formation of ultrafine scale structures in aluminium containing small amounts of particles by conventional rolling deformation

Y. D. HUANG*‡
Department of Materials Science and Engineering, University of Science and Technology Beijing, Beijing 100083, People's Republic of China; Department MTM, Katholieke Universiteit Leuven, Kasteelpark Arenberg 44, B-3001 Heverlee, Belgium
E-mail: Yuanding.Huang@mtm.kuleuven.ac.be

Y. L. LIU
Materials Research Department, Risø National Laboratory, DK-4000 Roskilde, Denmark

P. WAMBUA
Department MTM, Katholieke Universiteit Leuven, Kasteelpark Arenberg 44, B-3001 Heverlee, Belgium

The development of deformation microstructures during rolling has been studied in polycrystalline aluminium containing 0.8 vol.% of small Al_2O_3 particles and 2 vol.% of SiC whiskers. The morphology, size and misorientation of the ultrafine scale structures as a function of the imposed strain were characterised using transmission electron microscopy (TEM) technique. The observations were compared to those of cold rolled particle-free pure aluminium reported in the literature. The presence of particles enhances the rate and changes the nature of the development of the overall microstructure in comparison with pure aluminium. With the addition of second phase to pure aluminium, the ultrafine scale microstructure with its size less than 0.5 μm and a fraction of high angle boundaries greater than 30% can be obtained at a comparatively low strain of 2.7. In contrast, complicated processes or severe deformation with a strain of more than 5 are required for obtaining such structures in pure aluminium. The results indicate that there is a considerable potential for extending the present investigation to other particle-containing materials. By selecting second phases with suitable particle size and volume fraction and deformation processes one can expect to develop composites with ultrafine scale microstructure at a comparatively low strain.

1. Introduction

Among all the strengthening methods for metallic materials, the microstructural refinement appears to be the most promising to increase both the room temperature strength and ductility. Moreover, some specific features of mechanical behaviours, e.g. extremely high hardness and strength, lower temperature superplasticity and deviation from the Hall-Petch relationship, can be achieved by microstructural ultrafining. A lot of world-wide interest has been focused on how to obtain such ultrafine microstructure. Recent efforts, for example the application of inert gas condensation, mechanical alloying, heavy or severe plastic deformation and crystallisation from amorphous solids, have resulted in developing ultrafine grained (less than 1 μm) materials [1–7]. However, some difficulties still remain for these techniques to be used in industry on a large scale because of their limitations and high cost. It is very intriguing that in the latest years a ferrite grain around 1 μm has been obtained in plain carbon steels by a conventional rolling process (close to industrial production) with the usage of alloying, strain induced transformation and dynamic recrystallization of ferrite [8, 9].

It was reported that the existence of the particles in aluminium not only introduces structural inhomogeneities but also enhances the overall microstructural evolution when the material is deformed [10, 11]. This implies that the microstructural refinement can be attained in such particle-containing aluminium at a comparatively low strain by a conventional rolling process, while the same is difficult for pure aluminium unless special deformation processes and very high

*Author to whom all correspondence should be addressed.
‡*Present Address*: Department MTM, Katholieke Universiteit Leuven, Kasteelpark Arenberg 44, B-3001 Heverlee, Belgium.

TABLE I Microstructural parameters for the materials used

	Particle shape	Particle size	Particle spacing[a]	Volume fraction of particles (%)	Initial grain size (μm)
Al_2O_3	Plate	$d = 52$ nm $t = 8$ nm			
SiC_w	Cylinder	$d = 1$ μm $l = 6$ μm			
Al-Al_2O_3			Al_2O_3: 0.24 μm	Al_2O_3: 0.8	1116 ± 113
Al-Al_2O_3-SiC_w			SiC_w: 3.4 μm Al_2O_3: 0.24 μm	SiC_w: 2 Al_2O_3: 0.8	560 ± 42

[a]calculated value, d: diameter of plate or cylinder, t: thickness of plate, l: length of cylinder.

strains are applied. In an attempt to explore this possibility, the present work is carried out to investigate the microstructural evolution of two commercially pure aluminium alloys containing small amounts of particles, i.e. fine Al_2O_3 and large SiC_w whiskers, during cold rolling to a true strain up to 2.7. The deformation microstructure was characterized by trasmission electron microscopy (TEM). A Kikuchi pattern technique developed in recent years was applied to quantify the distribution of boundary misorientation [12].

2. Experimental procedures

The materials used were fabricated by powder route from Al powder with and without the addition of 2% by volume of SiC_w. The atomised aluminium powder had an average particle size of 6.4 ± 0.2 μm and was commercially pure containing no more than 0.26 wt% Fe and 0.18 wt% Si. The oxide from the surface of the Al powder appeared in the material as small Al_2O_3 particles of 0.8% by volume. The SiC_w, supplied by Mandoval Ltd., UK, had a mean diameter of 1 μm and a mean aspect ratio of about 6–7 in the composites.

The aluminium powder, both with and without SiC_w, was cold and hot compacted, then extruded at 500°C with an extrusion ratio of 15:1. The starting materials were made by cold rolling to 50% reduction in the original extrusion direction followed by annealing at 600°C for 24 h in vacuum. This treatment brought the materials to recrystallization [13].

The SiC_w, present as single whiskers and as small groups, was fairly uniformaly distributed and highly aligned with the extrusion-rolling direction. The Al_2O_3 particles were uniformly dispersed but a fraction of them was present in stringers approximately aligned with the extrusion-rolling direction. The parameters of the second phases and the initial grain sizes of the Al-Al_2O_3 and Al-Al_2O_3-SiC_w are given in Table I.

The starting materials were then deformed by cold rolling to 50% and 90% reduction in thickness, corresponding to the von Mises strain 0.8 and 2.7, respectively. Foils taken from longitudinal sections were prepared for TEM using a standard window electropolishing technique. TEM was performed using a JEOL 2000FX. The microstructure on the longitudinal plane was observed. Subgrain aspect ratio (dimension parallel to the rolling direction/dimension normal to the rolling direction) and size were measured on the micrographs. More than two hundred subgrains, including the subgrains near SiC_w and in the matrix, were analyzed. Crystallographic orientations of the subgrains were determined by the Kikuchi pattern techniques in the TEM [12], and then the misorientations across the subgrain boundaries were calculated as angle/axis pairs. About 100 to 150 boundaries were analyzed for each specimen. The subgrain boundaries analyzed included those near particles and those in the matrix.

3. Results

3.1. Al-Al_2O_3

For the specimen strained to 0.8, the structures (Fig. 1a) consist of cells/subgrains. Some of them are nearly equiaxed while others are elongated in the rolling direction. The average aspect ratio is 1.41 (Table II). Most of the Al_2O_3 particles lay on dislocation walls indicating that the position of the walls is influenced by the presence of the Al_2O_3 particles. Extended dislocation boundaries such as microbands characteristic for the structure of cold rolled pure Al are not found in the present specimen. The subgrain size distribution ranges from 0.2 to 1.6 μm. Large and small cells/subgrains are randomly distributed through the structure. The distribution of the misorientation across the subgrain boundary is below 14° with a single peak at 3° (Fig. 2a). There is no indication of the formation of the ultrafine grain at this strain (0.8).

In the specimen strained to 2.7 the structures (Fig. 1b) are comparable to those observed in the specimen strained to 0.8 (Fig. 1a). The differences are: the subgrain walls are sharper, subgrain size is smaller, size distribution is narrower and the misorientation is larger (Table II and Fig. 2a and 2b). The misorientation

TABLE II Average subgrain aspect ratio, size and misorientation

Materials	Strain	Subgrain aspect ratio	Subgrain size (μm)	Misorientation across sub-boundary (°)
Al-Al_2O_3	0.8	1.41	0.76 ± 0.02	4.5 ± 0.3
	2.7	1.51	0.44 ± 0.01	15.0 ± 2.5
Al-Al_2O_3-SiC_w	0.8	1.37	0.45 ± 0.02	12.4 ± 1.8
	2.7	1.69	0.39 ± 0.01	21.3 ± 2.3

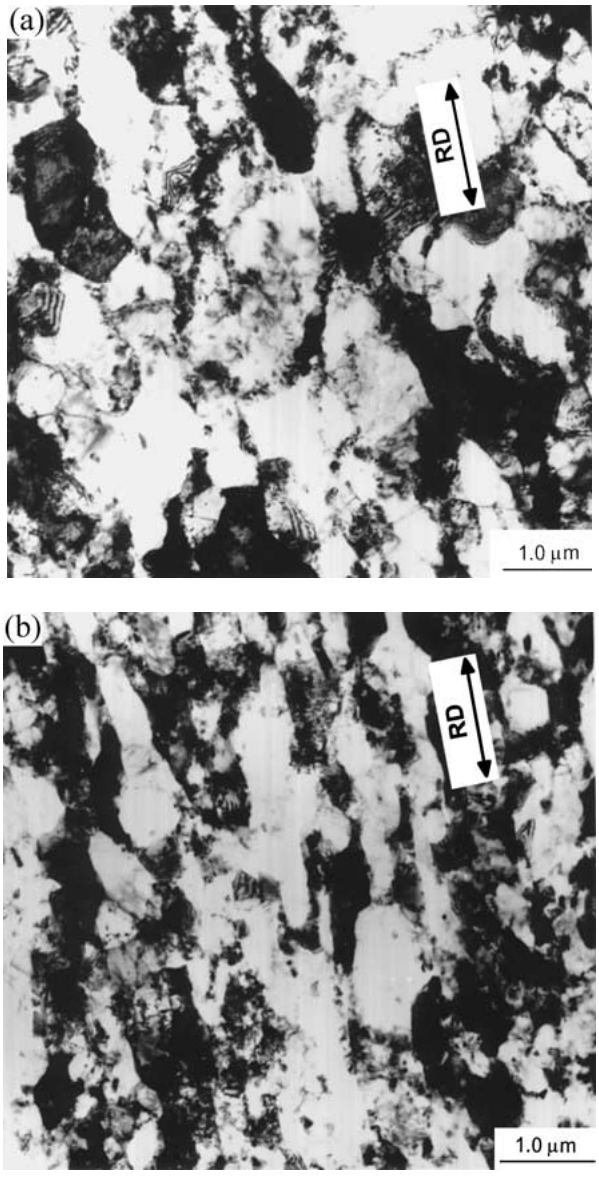

Figure 1 TEM micrographs showing the microstructure of the cold rolled Al-Al_2O_3, (a) $\varepsilon = 0.8$, and (b) $\varepsilon = 2.7$. The rolling direction (RD) is marked on the micrographs using an arrow.

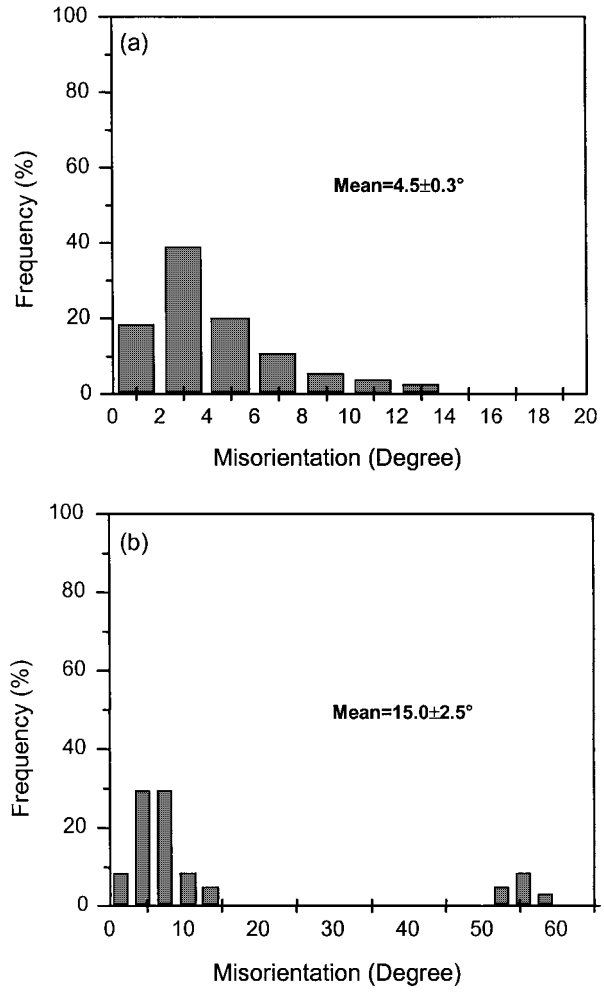

Figure 2 Distribution of misorientation across subgrain boundary in the cold rolled Al-Al_2O_3, (a) $\varepsilon = 0.8$, and (b) $\varepsilon = 2.7$.

distribution with an average of $15.0 \pm 2.5^\circ$ becomes a bimodal type and the fraction of high angle boundaries (>15°) is 17%, indicating that a fraction of ultrafine grains may form (hereafter, this part of microstructure with a misorientation more than 15° is termed ultrafine grained microstructure). The average subgrain aspect ratio is slightly increased (Table II). Most of the elongated subgrains are associated with the highly aligned bands of Al_2O_3 particles. The formation of such elongated subgrains may be attributed to: 1) the increasing deformation, bands of Al_2O_3 particles becoming more highly aligned, and 2) the interaction between dislocation walls and Al_2O_3 particles. However, the chance of finding high angle boundaries in line-scan parallel to the rolling direction equals to that normal to the rolling direction, indicating that the structure is non-directional.

3.2. Al-Al_2O_3-SiC_w

The large amount of cells and subgrains, and small amount of dislocations which tangle each other within the cells/subgrains coexists in the specimen deformed to 0.8 (Fig. 3a). The region of well defined subgrains extends out from SiC_w into the matrix. The subgrain size near SiC_w is smaller (0.2–0.3 μm) than that in the matrix which consists of a random mixture of large and small cells/subgrains (Fig. 3b). The average size is 0.45 ± 0.02 μm (Table II). The cells/subgrains have an aspect ratio of 1.37. They appear to be more equiaxed in regions near SiC_w and SiC_w groups than in the matrix. Similar to Al-Al_2O_3 no extended boundary is found in the structure. The misorientation distribution with an average of $12.4 \pm 1.8^\circ$ appears a bimodal type (Fig. 4a). The fraction of the high angle boundaries with the misorientation more than 15° is about 22%. In contrast to Al-Al_2O_3 materials deformed to the same strain, the high angle boundaries can be formed at a lower strain in Al-Al_2O_3-SiC_w and they are frequently found in the regions near SiC_w, indicating that the addition of large size SiC_w promotes the formation of high angle boundaries. But at this stage their spatial distribution is not homogeneous.

At the strain of 2.7, the well-defined subgrains with sharp boundaries dominate the microstructure (Fig. 3c). As compared with the specimen strained to 0.8, the subgrain size near SiC_w is basically unchanged, the subgrain size in the matrix decreases and the variation in subgrain size throughout the material becomes less

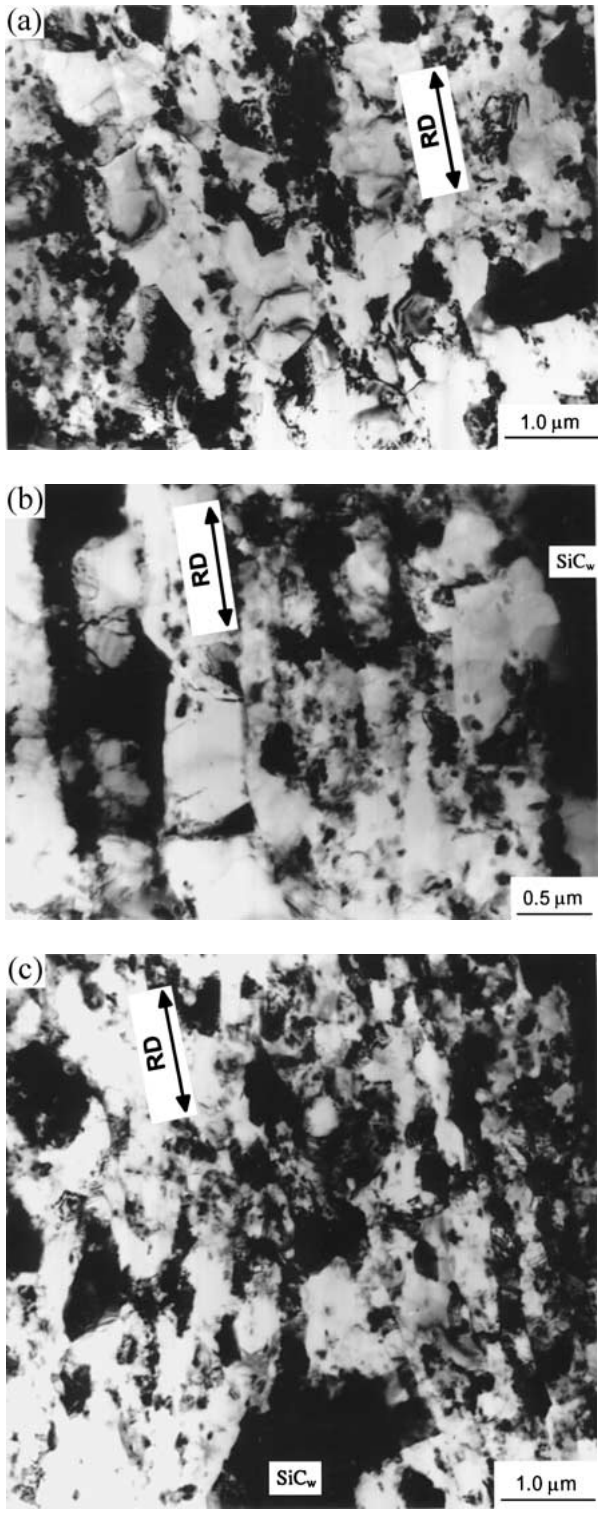

Figure 3 TEM micrographs showing the microstructure of the cold rolled Al-Al_2O_3-SiC_w, (a) $\varepsilon = 0.8$, the general microstructure, (b) $\varepsilon = 0.8$, the subgrains near SiC_w and in the matrix, and (c) $\varepsilon = 2.7$. The rolling direction (RD) is marked on the micrographs using an arrow. SiC_w: SiC whisker.

significant. The average size is decreased to 0.39 ± 0.01 μm. The subgrain aspect ratio is increased to 1.69 (Table II). The considerably elongated subgrains are usually found in the regions free of SiC_w and are associated with the highly aligned bands of Al_2O_3 particles. In this deformed specimen the fraction of high angle boundaries is increased to 35%. The average misorientation is $21.3 \pm 2.3^\circ$ (Table II and Fig. 4b). Unlike the

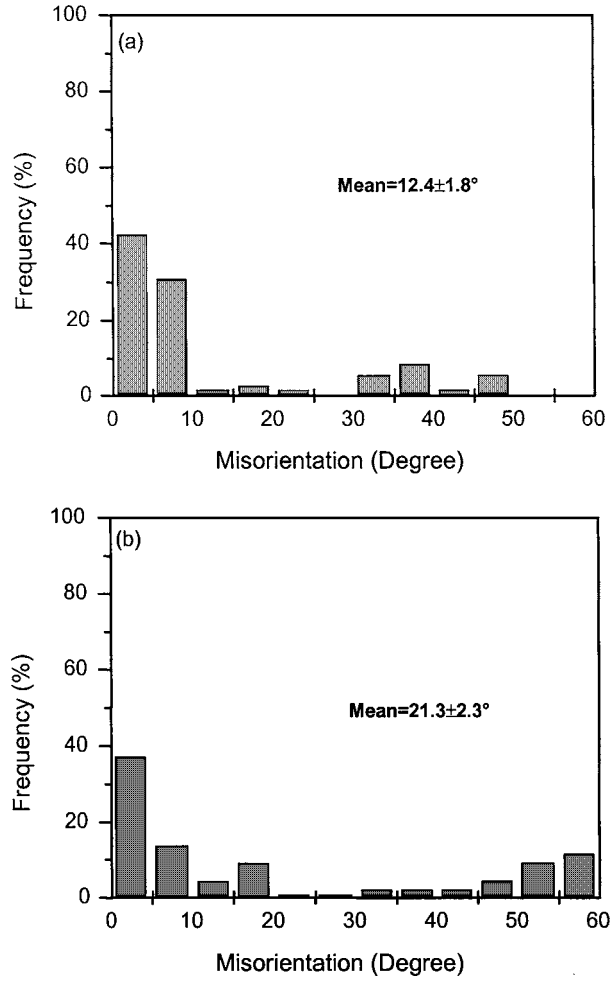

Figure 4 Distribution of misorientation across subgrain boundary in the cold rolled Al-Al_2O_3-SiC_w, (a) $\varepsilon = 0.8$, and (b) $\varepsilon = 2.7$.

specimen deformed to 0.8, many high angle boundaries are also found in the matrix.

The misorientation measurement further confirms that the structure is non-directional at the strains of 0.8 and 2.7. The average misorientation in line-scan parallel to the rolling direction equals to that normal to the rolling direction.

4. Discussion

In the range of true strains investigated, the subgrains, cells and ultrafine grained microstructure coexist in both the Al-Al_2O_3 and Al-Al_2O_3-SiC_w. With increasing strain the structure is rapidly refined and the fraction of high angle boundaries is increased. An ultrafine scale structure with a spacing less than 1 μm and a fraction of high angle boundaries greater than 30% is obtained by a strain of 2.7. It was reported that to obtain a similar ultrafine microstructure in pure Al, Cu, Fe, Ni, Mg, Ti and single phase Al-0.13% Mg, complicated deformation path (fx. by equal-channel angular pressing) and higher strains of 5 or more are required [2, 4, 6, 7]. The present work demonstrates that the presence of 0.8 vol% Al_2O_3 particles or of a combination of 0.8 vol% Al_2O_3 and 2 vol% SiC_w is rather efficient in refining the microstructure of the Al matrix during cold rolling. The introduction of 0.8 vol% Al_2O_3 particles in

pure aluminium is beneficial to obtaining a uniformly distributed ultrafine grained microstructure at a strain of about 2.7. The addition of 2 vol% SiC_w further lowers the strain to about 0.8 at which the ultrafine grained structure forms.

4.1. Microstructural evolution

In the following paragraphs the microstructural evolution of the two materials studied is dicussed in respect to the rate and morphology as compared to pure aluminium.

The measured mean subgrain size, the mean misorientation and the fraction of high angle boundaries as functions of the von Mises strain for the two materials studied are summarised in Figs 5–7, respectively. The data for aluminium reinforced with particles Al_2O_3 and SiC_w cold rolled to 0.2 and pure Al [14–18] is also included for comparison. It is clearly shown that the presence of Al_2O_3 particles reduces the subgrain size and increases the mean misorientation and the angular spread at a given strain. The addition of SiC_w further changes the microstructure in the same direction. The effects on enhancing microstructural evolution of these two particles are attributed to the higher dislocation density introduced as thermal dislocations in the starting materials and introduced during deformation [19, 20].

It is noted that the effects of Al_2O_3 particles and SiC_w on reducing subgrain size are more significant in the low strain range (<0.8) and become smaller with increasing strain (see Fig. 5). In fact, the subgrain size of the Al-Al_2O_3-SiC_w appears to have reached a limiting value (0.4 μm) at the strain of 0.8. Subgrain size saturation has also been observed in a cold rolled Al-3.8 vol% Al_2O_3 [21], whereas no limiting value of the spacing between lamellar boundaries was reported in a commercially pure Al cold rolled up to a very large strain of 5.0 [18]. The subgrain size saturation at relatively low strains is characteristic in particle-containing materials. This phenomenon is believed to be related to higher recovery rates in these materials as a result of more dislocation interaction, higher point defect density and higher diffusion rates [21, 22].

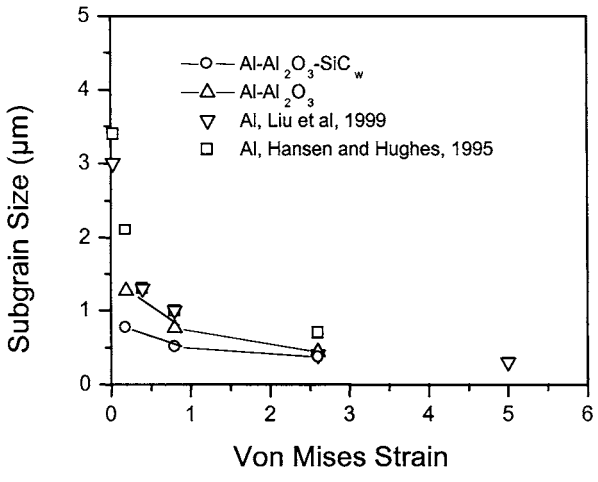

Figure 5 Mean subgrain size as a function of von Mises strain in the cold rolled Al-Al_2O_3 and Al-Al_2O_3-SiC_w. The data of cold rolled pure Al is included for comparison.

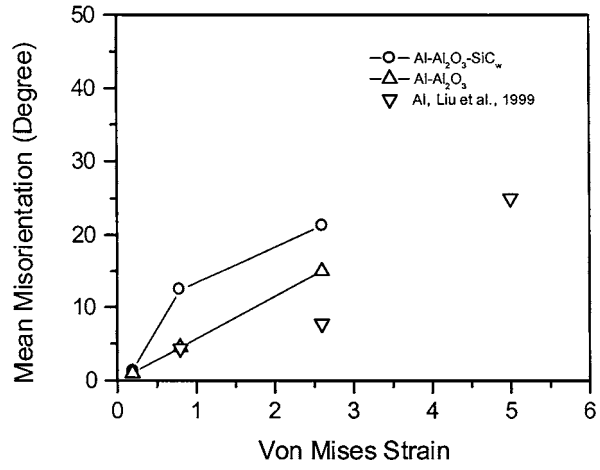

Figure 6 Mean misorientation as a function of von Mises strain in the cold rolled Al-Al_2O_3 and Al-Al_2O_3-SiC_w. The data of cold rolled pure Al is included for comparison. Note the misorientation measured in the pure Al is that of lamella boundaries.

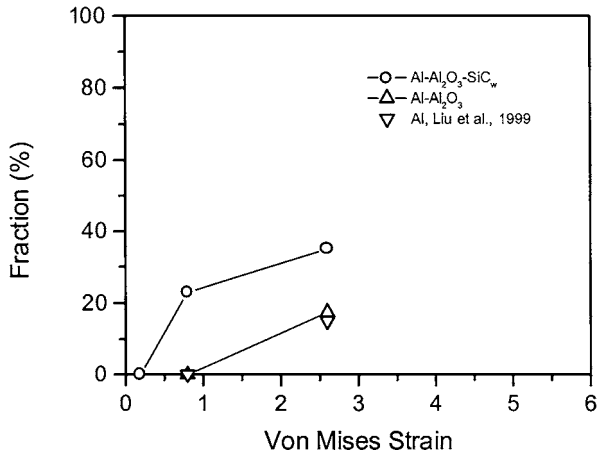

Figure 7 Fraction of high angle boundaries (>15°) as a function of von Mises strain in the cold rolled Al-Al_2O_3 and Al-Al_2O_3-SiC_w. The data of cold rolled pure Al is included for comparison.

It is known that the misorientation in cold rolled pure Al increases continuously with strain up to very large strains. The addition of Al_2O_3 particles and SiC_w increases the rate of the misorientation development (Figs 6 and 7). But, unlike the development of subgrain size, no saturation value of misorientation has been found in the strain range investigated. The strong effect of SiC_w is indicated by the fact that the presence of SiC_w lowers the strain level at which high angle boundary starts to form. At the strain of 0.8, the angular spread in the Al-Al_2O_3-SiC_w (high angle boundary fraction is 22%) is comparable to that of Al-Al_2O_3 and of pure Al at the strain of 2.7 (high angle boundary fraction is 17–18%) (Figs 2, 4, 6 and 7). It is also noted that the presence of Al_2O_3 and SiC_w changes the spatial distribution of high angle boundaries. There does not seem to be a correlation between the boundary misorientation and the geometrical orientation of the boundary within the sample. This contrasts with the observations in pure Al, where most of high angle boundaries are associated with the lamellar boundaries parallel to the rolling plane [14–18].

As mentioned above, the microstructure of cold rolled Al-Al_2O_3 and Al-Al_2O_3-SiC_w in the whole strain range studied is characterised by the formation of a mixed structure of cells/subgrains with randomly distributed high angle boundaries. These structures are strikingly different from those of the cold rolled particle-free pure Al. In the latter structural features with preferential directions such as microbands (MBs) and lamellar structures are dominating [14–18]. These band structures are indications of a long range slip pattern. They are typical resulting from deformation with a reduced number of slip systems in single-phase polycrystals, in which strain compatibility is achieved by subdividing individual grains into cell blocks with deformation induced dislocation boundaries.

Under room temperature deformation the microstructural transition from a band structure to an equiaxed structure is generally a consequence of an increase in the number of simultaneously active slip systems [23]. The present work shows that the presence of 0.8 vol% Al_2O_3 particles alone and the presence of 0.8 vol% Al_2O_3 + 2 vol% SiC_w change the slip pattern and break down the band structures. For Al_2O_3 particles this may be a consequence of the secondary slip which takes place near the particles. The secondary dislocations act as obstacles to primary slip and cause a change in the overall deformation pattern compared with the behaviour of the particle-free material [21]. Adding 2% SiC_w may further increase the number of active slip systems required for strain accommodation in the vicinity of SiC_w.

4.2. Industrial relevance

There is considerable interest currently in refinement of deformation microstructures in order to optimise the yield stress without impairing toughness. Although the ultrafine grained microstructure has been achieved in pure metals or single-phase alloys by severe deformations, the technical processes involved are very costly from energy and productivity point of view. The present investigation supplies an alternative approach to obtain the ultrafine scale microstructures at a comparatively low strain. This could open the way to low-cost production of these highly refined materials. It can be expected that the combination of the suitable additions of fine second phases in aluminium with the conventional process, such as rolling, will permit us to obtain new alloys of unusual composition and to produce new ultrafine scale metal-ceramic composites. It is also believed that the fraction of the high angle grain boundaries increases in the overall deformed microstructure and the strain needed to obtain the ultrafine scale microstructure decreases with increasing volume fraction of the second phase. In fact, the average misorientation increases up to around 30° for an aluminium containing 3.8 vol.% fine alumina particles at the strain range from 2.3 to 3.0 with a fraction of high angle boundaries about 60%. The average size of the ultrafine microstructure is about 0.15 μm [21, 22].

5. Conclusions

1. An ultrafine scale microstructure in aluminium containing 0.8 vol% of Al_2O_3 and 2 Vol% of SiC_w is achieved by cold rolling to a strain of 2.7. This structure is defined as a mixture of small cells and subgrains (<0.5 μm) with many randomly distributed high angle boundaries (fraction 17–35%). To obtain a similar structure in pure aluminium, complicated processes and severe plastic deformations are required. The different behaviour is attributed to the following:

- The microstructural evolution is accelerated by the presence of Al_2O_3 particles and further by the combination of Al_2O_3 and SiC_w. Such acceleration is nonexistent in particle-free aluminium. In the Al-Al_2O_3-SiC_w a limiting subgrain size is reached by the strain of about 0.8 indicating higher dislocation density, more pronounced recovery and a faster trend of attaining low-energy states. But a steady state has not been reached in the strain range investigated as the average misorientation continues to increase with strain.
- The presence of the small Al_2O_3 particles and SiC_w changes the slip pattern of the matrix and the resulting microstructure is different by nature from that of particle-free aluminium. Instead of developing bands and lamellae, the microstructure is rapidly broken up and refined.

2. The present investigation provides an alternative approach to obtain ultrafine scale microstructures at a comparatively low strain. This could open the way to low-cost production of these highly refined materials.

Acknowledgements

The authors wish to thank Dr. N. Hansen for encouragement and support, Drs. C. Y. Barlow, Q. Liu and X. Huang for fruitful discussions, P. Nielsen and J. Lindbo for expert assistance in the experimental work. Y. D. Huang is grateful to the Danish International Development Assistance (DANIDA) for the financial support.

References

1. R. BIRRINGER and H. GLEITER, "Encyclopedia of Materials Science and Engineering, Supplement 1" (Pergamon, London, 1988) p. 339.
2. J. R. BOWEN, P. B. PRANGNELL and F. J. HUMPHREYS, in Proceedings of the 20th Risø International Symposium on Materials Science: Deformation-induced Microstructures: Analysis and Relations to Properties, Risø National Laboratory, Roskilde, Denmark, edited by J. B. Bilde-Soerensen, J. V. Carstensen, N. Hansen, D. J. Jensen, T. Leffers, W. Pantleon, O. B. Pedersen and G. Winther (1999) p. 269.
3. F. H. FROES and C. SURYANARAYANA, *J. Met.* **6** (1989) 12.
4. Y. IWAHASHI, Z. HORITA, M. NEMOTO and T. G. LANGDON, *Acta Mater.* **46** (1998) 3317.
5. C. C. KOCH and Y. S. CHO, *Nanostruct. Mater.* **1** (1992) 207.
6. A. A. POPOV, I. Y. PYSHMINTSEV, S. L. DEMAKOV, A. G. ILLARIONOV, T. C. LOWE, A. V. SERGEYEVA and R. Z. VALIEV, *Script Materialia* **37** (1997) 1089.
7. R. Z. VALIEV, A. V. KORZNIKOV and R. R. MULYUKOV, *Mater, Sci. Eng.* **A168** (1993) 141.
8. Y. MATSUMURA and H. YADA, *Trans. ISIJ* **27** (1987) 492.

9. P. D. HODGSON, M. R. HICKSON and R. K. GIBBS, *Mater. Sci. Forum* **284–286** (1998) 63.
10. F. J. HUMPREYS, *Met. Sci* (1979) 136.
11. C. Y. BARLOW and N. HANSEN, *Acta Mater*. **39** (1991) 1971.
12. Q. LIU, *Ultramicroscopy* **60** (1995) 81.
13. Y. L. LIU, N. HANSEN and D. J. JENSEN, *Met. Trans.* **20A** (1989) 1743.
14. N. HANSEN and D. A. HUGHES, *Phys. Stat. Sol.* **149B** (1995) 155.
15. N. HANSEN, in Aluminum Alloys for Packagings II, Warrendale, PA, US, edited by J. G. Morris (The Minerals, Metals and Materials Society, Materials Park, OH, 1996) p. 11.
16. D. A. HUGHES and N. HANSEN, *Acta Mater*. **45** (1997) 3871.
17. Q. LIU AND N. HANSEN, *Phys. Stat. Sol*. **149B** (1994) 187.
18. Q. LIU, X. HUANG, D. J. LIOYD and N. HANSEN, in 4th Int. Conf. on Recrystallization and Related Phenomena, edited by S. Sakai and H. G. Suzuki (Japan Inst. of Metals, 1999) p. 315.
19. R. J. ARSENAULT and N. SHI, *Mater. Sci. Eng*. **A81** (1986) 175.
20. M. F. ASHBY, *Phil. Mag*. **21** (1970) 399.
21. C. Y. BARLOW and Y. L. LIU, in Proceedings of the 20th Risø International Symposium on Materials Science: Deformation-Induced Microstructures: Analysis and Relations to Properties, Risø National Laboratory, Roskilde, Denmark, edited by J. B. Bilde-Soerensen, J. V. Carstensen, N. Hansen, D. J. Jensen, T. Leffers, W. Pantleon, O. B. Pedersen and G. Winther (1999) p. 261.
22. C. Y. BARLOW, N. HANSEN and Y. L. LIU, *Acta Mater.*, in press.
23. X. HUANG and N. HANSEN, *Scripta Mater.* **37** (1997) 1.

Received 3 August 2000
and accepted 7 May 2001